Hunting for intermediate black holes - Andrija Kostić

June 6, 2018

1 Introduction

Following the work on observations and data reduction (Bellini et al. [4]; Baldwin et al. [5]; Watkins et al. [6];), made possible by high precision Hubble Space Telescope (HST) proper motion measurements, it was possible to resolve individual stars and further constrain the properties of observed globular clusters. With this advantage at hand, it is now possible to discretely model the globular clusters, taking care of each given star separately. This approach has an advantage over previously used methods (binning the field of view), because it doesn't cause a loss of precious information given by the observations. Using the likelihood analysis incorporated with Jeans modelling, Watkins et al. [2] were able to make a dynamical model of the ω Cen globular cluster, and reproduce it's properties in agreement with previous studies. The previous research encouraged a further effort in reducing the amount of assumptions needed for feasible modeling of these complex stellar systems and hence enriching the available technique. Bianchini et al. [1], introduced a new analytic function which is able to cover and describe the dispersion profile of the whole range of stellar populations inside the globular cluster:

$$\sigma(m) = \begin{cases} \sigma_0 \exp(-\frac{1}{2}\left(\frac{m}{m_{eq}}\right)), & \text{if } m < m_{eq} \\ \sigma_{eq}\left(\frac{m}{m_{eq}}\right)^{-1/2}, & \text{if } m > m_{eq}, \end{cases}$$

where the m_{eq} represents the mass of a star which is in full equipartition, and hence has a qualitative and physical weight in describing the cluster state, along with σ_0 which represents the dispersion of star with a mass $m = 0$. The dependence $\sigma(m)$ was known previously to exist, but the correct dependence was unknown (Trenty and van der Marel [8]). Due to lack of observational data and computing power, people didn't account for this in their analysis. Now, with the presence of state of the art likelihood analysis tools like the `emcee` code (Foreman D. et al [7]) and available CPU and GPU computing power, it is possible to construct more detailed models and enhance the current knowledge about these stellar systems. The goal of this summer project was to incorporate the proposed $\sigma(m)$ from Bianchini et al. [1] dependence into the existing Jeans modeling code developed by Watkins et al. [2] (`CJAM` code) and use the `emcee` code in order to find the appropriate m_{eq} parameter for the cluster of interest. With this m_{eq} parameter determined, one could make conclusions on other relevant cluster properties and determine it's dynamical state, and perhaps make some constraints on the presence of intermediate black holes (IMBHs) in the centers of observed clusters.

2 Modelling the cluster

Before applying developed models to the observational data it is necessary to filter out any bad ideas, and hence we used the simulation data provided by Downing et al. [9] and tried to make our models work on this data set.

Analysing the dynamical structure of globular clusters with the `CJAM` code[1] requires some input information of it's potential. Because it is nearly impossible to obtain intrinsic density

[1] It should be noted, that by dynamical modelling here, we mean on deducing the moments (first and second) of the stars, with which it is possible to tell the dynamical state and structure of the cluster.

distribution, and hence the intrinsic potential distribution of the globular cluster, one has to deal with projected quantities. The practical and efficient way of representing the projected density distribution of the globular cluster is using multi gaussian expansions (MGEs). Using Capellari's code [3], we are able to produce luminous and mass MGEs of the simulated cluster (figure 1). This information on $\nu(r)$ (density distribution) and $l(r)$ (luminous density) is necessary for constraining distribution function $f(\vec{r}, \vec{v})$, which is in return used in limiting the possible values of clusters' potential $\Phi(r)$.

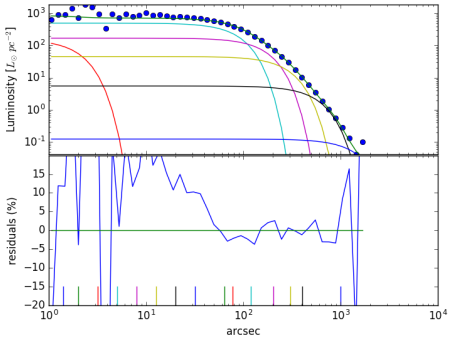

(a) Luminosity MGE

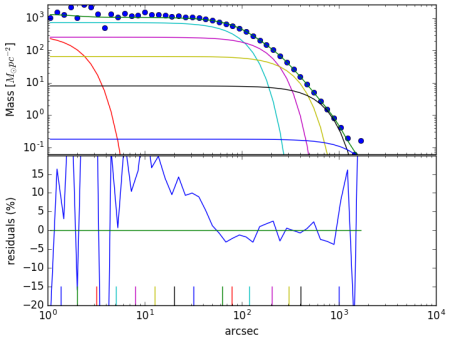

(b) Mass MGE

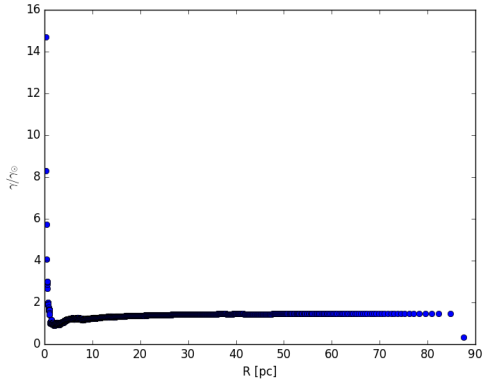

(c) Dependance of $M/L[M_\odot/L_\odot]$ with radius

Figure 1: MGE obtained with Cappelari's 1D MGE expansion code [3]

In practise, it is only possible to obtain the luminous MGE, because it is very hard to measure the mass of individual stars in the cluster. Here, the $l(r)$ and mass-to-light ratios give the information on $\nu(r)$. Further, by using this information and some additional assumptions on axisymetry, alignment of velocity elipsoid with chosen cylindrical coordinate system and constant anysotropy and mass-to-light parameter, it is possible to solve the Jeans equations for the second moments. The second moments directly infer the shape of the velocity elipsoid of the cluster, which in addition gives constraints to internal dynamics. In order to obtain a unique solution for the first moments also, an assumption for contributions of ordered and random motion to the velocity dispersion is needed (eq (22) in [2]). This assumption is incorporated into the code by assigning a rotation paramater κ to each luminous MGE. With the known first moments it is possible to make conclusions on internal rotation in the cluster as well construct the covariance matrix needed for likelihood analysis of the calculated moments (see [2] chap. 3). After one calculates first and second moments, it is possible to constrain the distribution function $f(\vec{r}, \vec{v}, t)$, which further, gives constraints on potential $\Phi(r)$.

In fig. 2 the difference between the projected and spherical velocity dispersion for the chosen simulation is shown. One would expect that in the outer shells there would be no difference, but it seems that for the Z-axis it is not the case (fig. 2c). This could imply some missunderstanding of the data.

Nonetheless, the performance of the `CJAM` code was tested with this data. The comparison of the model with the projected velocity dispersion calculated from the simulation is presented in the right column of fig. 3 (black is the model). Here, the input for the cjam were the positions of 5000 stars from the mean-mass range $(0.3 - 0.4M_\odot)$ within the $\approx 200''$. Reason for this is to simulate the observational conditions, because rarely is the data beyond the half-light radius obtained. One could notice that the model for the right input parameters gives the moments which are in agreement with the low mass-range end of the set $(0.1 - 0.2M_\odot)$.

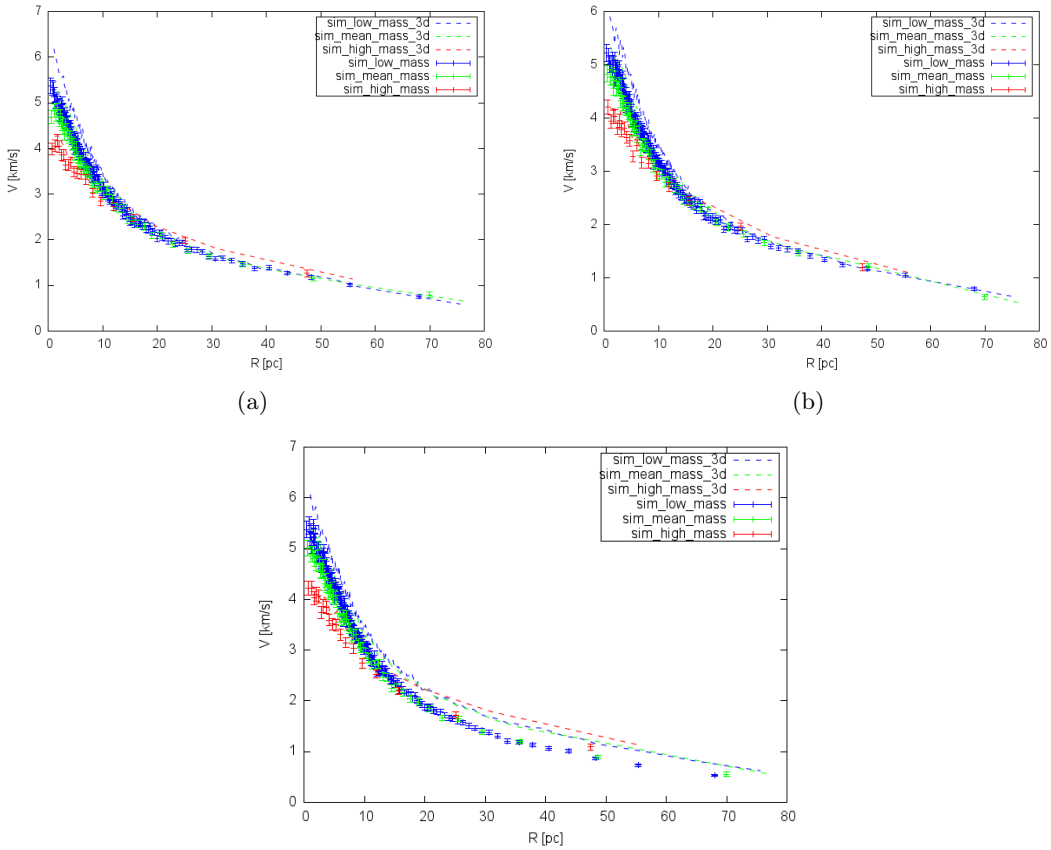

Figure 2: Here the velocity dispersions for different stellar masses for each axis are shown. From (a) to (c) are X,Y and Z-axis respectively. The colors corespond to different mass bins, red - high mass bin, blue - low mass bin and gree - mean mass bin. The simulation data (simulation one at 11Gyrs from [1]) was used in order to obtain these plots. The data points with error bars represent the data binned in the projection plane (in this case the X-Y plane of the simulation data), and the dashed lines represent the binning done in the spherical manner. The errors are calculated as the standard deviation of the mean for the data points in the selected bean, namely $\Delta\sigma = \sigma/\sqrt{N_{bin}}$. The odd thing is the disagreement in the plot with Z-axis dispersion shown. One would expect that the dispersion on the outher shells (3D-spherical) and rings (2D - projected) should be the same, as is the case fo X and Y-axis.

On the other hand, when Binachini's formula is implemented, model gets a lot better, and reproduces the dispersion for the right mass range (left column of figures in fig. 3. The only thing to worry about here is that the model finds parameters which are not in accordance to the ones calculated from the data. In other words, the parameters are $\beta_z \approx 0.0432$, $\kappa \approx 0.0929$, $M/L \approx 1.0808$, $i \approx pi/2$, distance $10kpc$, $\epsilon \approx 0$ and $\overline{m} \approx 1.1143$, while the m_{eq} parameter was kept fixed to $2M_{\odot}$. One could see from the emcee chain fig. 8 That it still hasn't converged, even though, the models get highly rated. Similiar thing happens with other runs (fig. 4, **??**).

Possible restriction which can be made is in the prior likelihood distribution. The emcee chain is restricted from below for $\overline{m}$ and m_{eq}, but not from above. The upper limit should be the physically meaningful one, for example, $\overline{m} < 1M_{\odot}$, because only the extreme cases of stars have masses bigger than $1M_{\odot}$ in the cluster, and $m_{eq} < 10$.

In order to see the behavior of emcee sampling, a run with only m_{eq} and $\overline{m}$ as free parameters is presented in the 4.4. Here the upper prior constraints are present. It could be seen that even for the right calculated parameters of the cluster, the chain quickly converges but has a quite dispersed sampling. Detailed description of the incorporation of equipartition into the `CJAM` is presented in the next chapter.

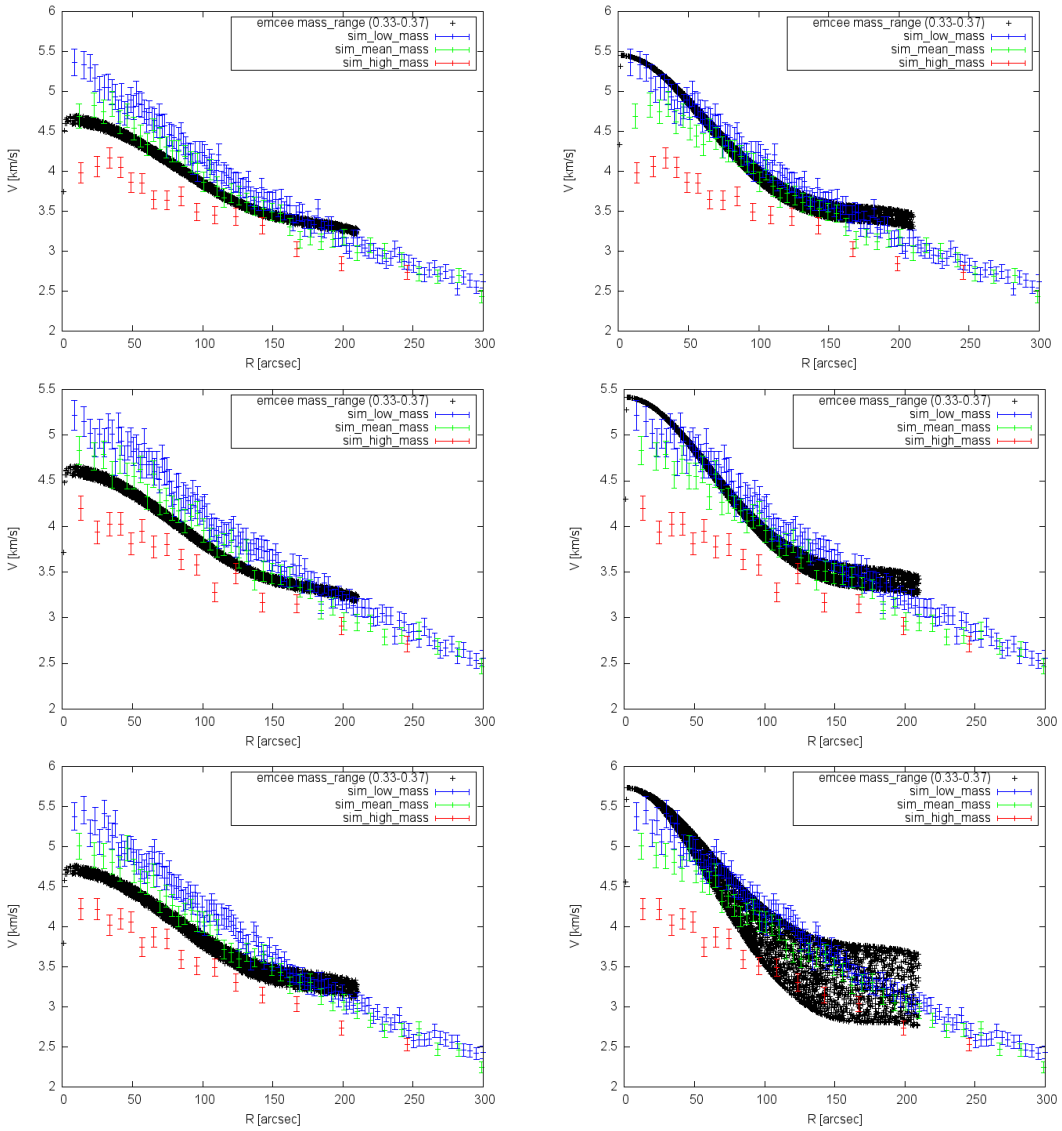

Figure 3: Using the *cjam* code developed by [2], one can try to model the dynamical state of the observed cluster. The figures in the right column are the ones which don't include modification with formula given by [1], and the ones on the left are the moments produced by the best model as found by emcee in the run 4.2. The color representation is the same as in figure fig. 2. The input parameters here are given in accordance to the calculated parameters of the simulated cluster, namely: (1) $\beta_z \approx 0.17$; (2) $\kappa \approx 0.0$; (3) $M/L \approx 1.47$ $[M_\odot/L_\odot]$; (4) $i \approx \pi/3$; (5) distance $\approx 10[kpc]$;. When it comes to the left column (4.2), the best model in the emcee chain finds the following: (1)$\beta_z \approx 0.0432$; (2) $\kappa \approx 0.0929$; (3) $M/L \approx 1.0808$; (4) $i \approx pi/2$ (5) distance $10kpc$; (6) $\epsilon \approx 0$; (6)$\overline{m} \approx 1.1143 M_\odot$. The MGEs needed for the model creation were calcualted using Capellari's 1D MGE expansion [3] and are shown in the figure 1. It seems that the model reproduces the best the high mass end of the stellar population. This is a rather strange result, because the input mass bin is, as it is also noted in the legends of the figures, $0.31 - 0.33[M_\odot]$.

3 Mass equipartition

As it was noted in section 3, the `CJAM` code assigns moments based on stars (x, y) positions, and then a separate code calculates the likelihood of this model being good. This is done in the approximation with gaussians (eq (12) from [2]). Only thing that is changed in this, for incorporation of equipartitioning formula, is the change of the dispersion used in the covariance matrix. Therefore eq. eq. (1) is used for the second moments in the covariance matrix from the

previously mentioned paper.

$$\sigma_{new}(m_i) = \sigma_{old}(\overline{m})exp(-\frac{1}{2}\frac{m_i - \overline{m}}{m_{eq}}), \tag{1}$$

where σ_{new} is the new 2nd moment assigned to a given star with mass m_i. An assumption that the initial model assigns σ_old 2nd moments to some mean mass star sample with a mass of $\overline{m}$ is made. Results of the chains and marginalized distribution probabilites are shown below.

3.1 Run 1: Both m_{eq} and $\overline{m}$ are kept free

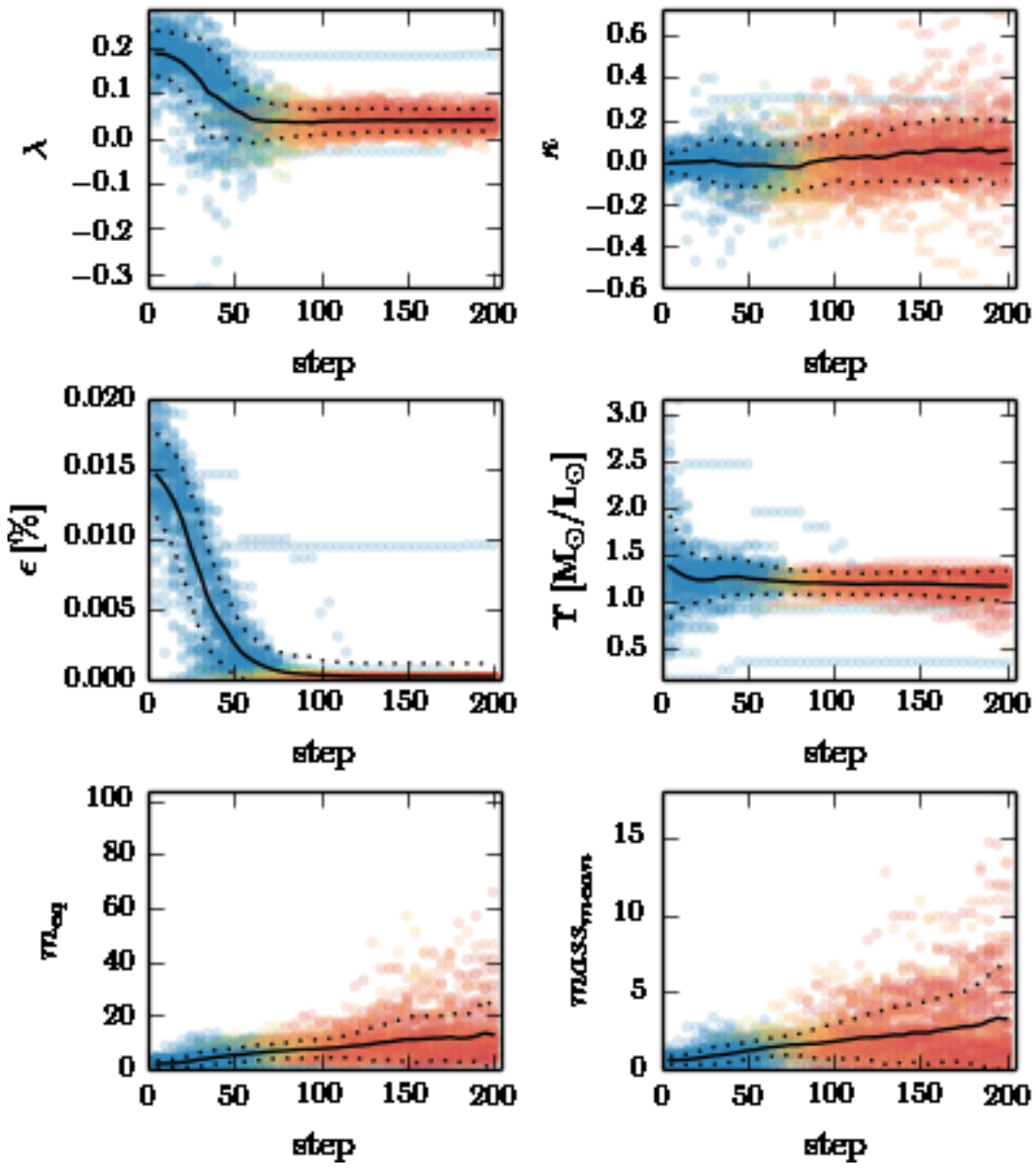

Figure 4: Here, all the parameters are set free for the emcee chain and its progress is shown. Eventhough the models get rated quite good (as they really are lying on the right mass range). The chain manages to converge on close to right values for M/L, ϵ and κ, but the anisotropy is lower than it was calculated for the simulation ≈ 0.17. Also, the m_{eq} and $\overline{m}$ are quite high.

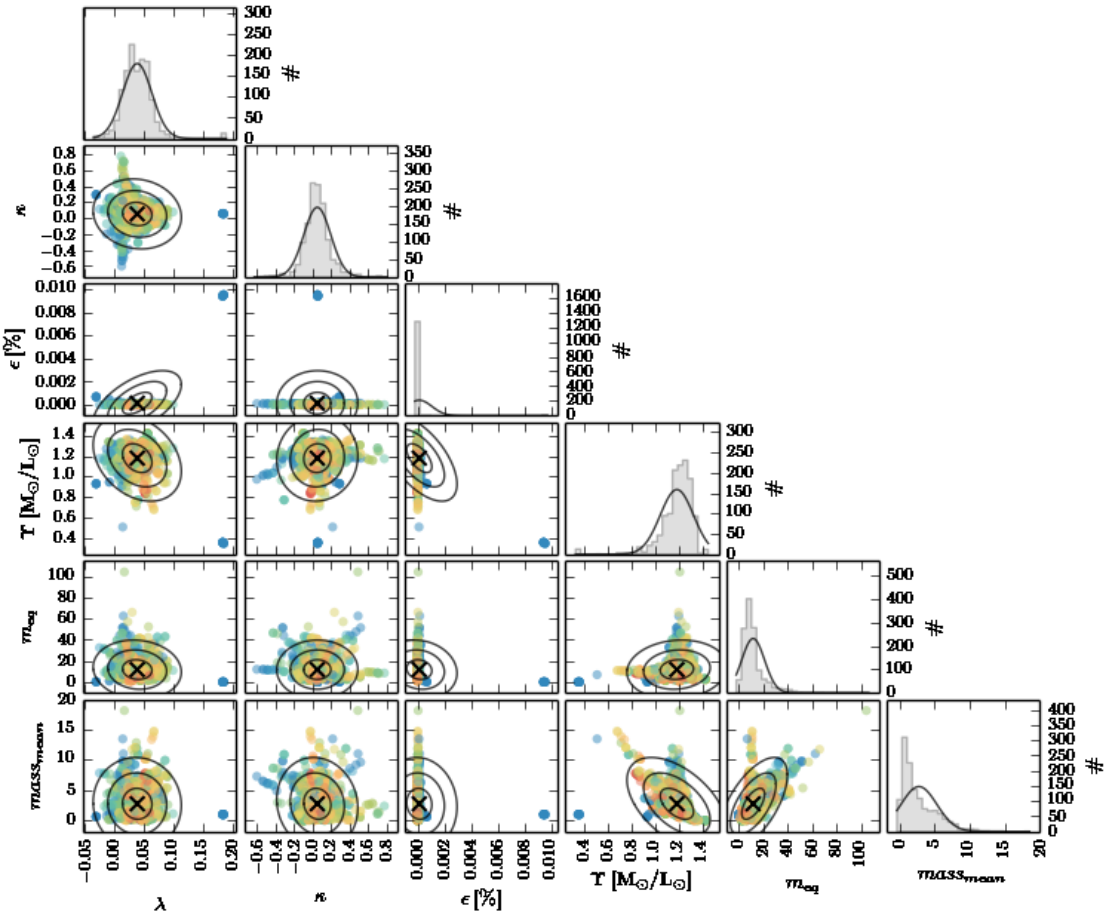

Figure 5: The distributions are presented in this figure.

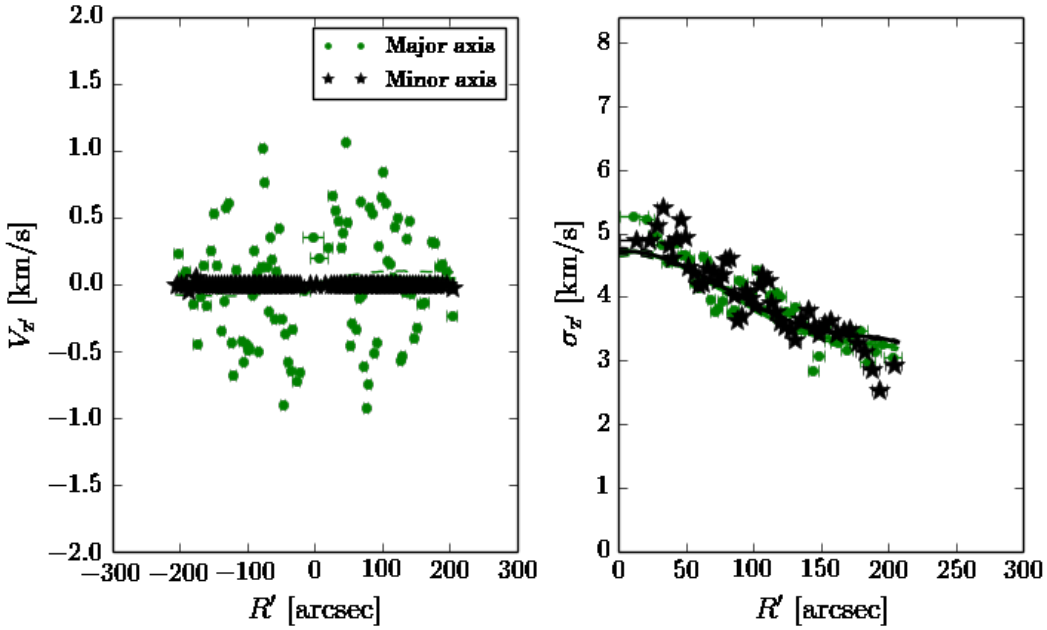

Figure 6: Overlayed input data, and the calculations of the best model from CJAM, as found by the chain.

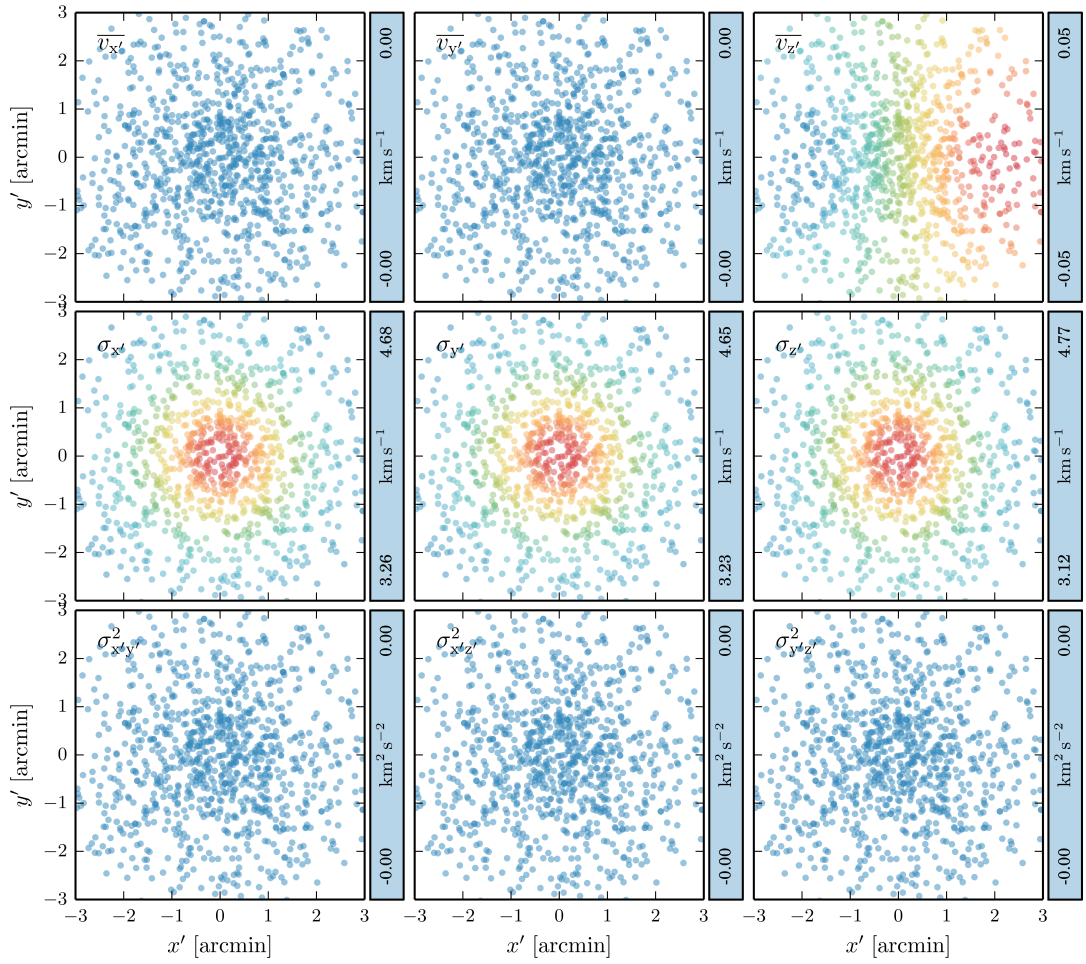

Figure 7: The proper motions.

3.2 Run 2: Only $\overline{m}$ is free parameter and m_{eq} is kept constant

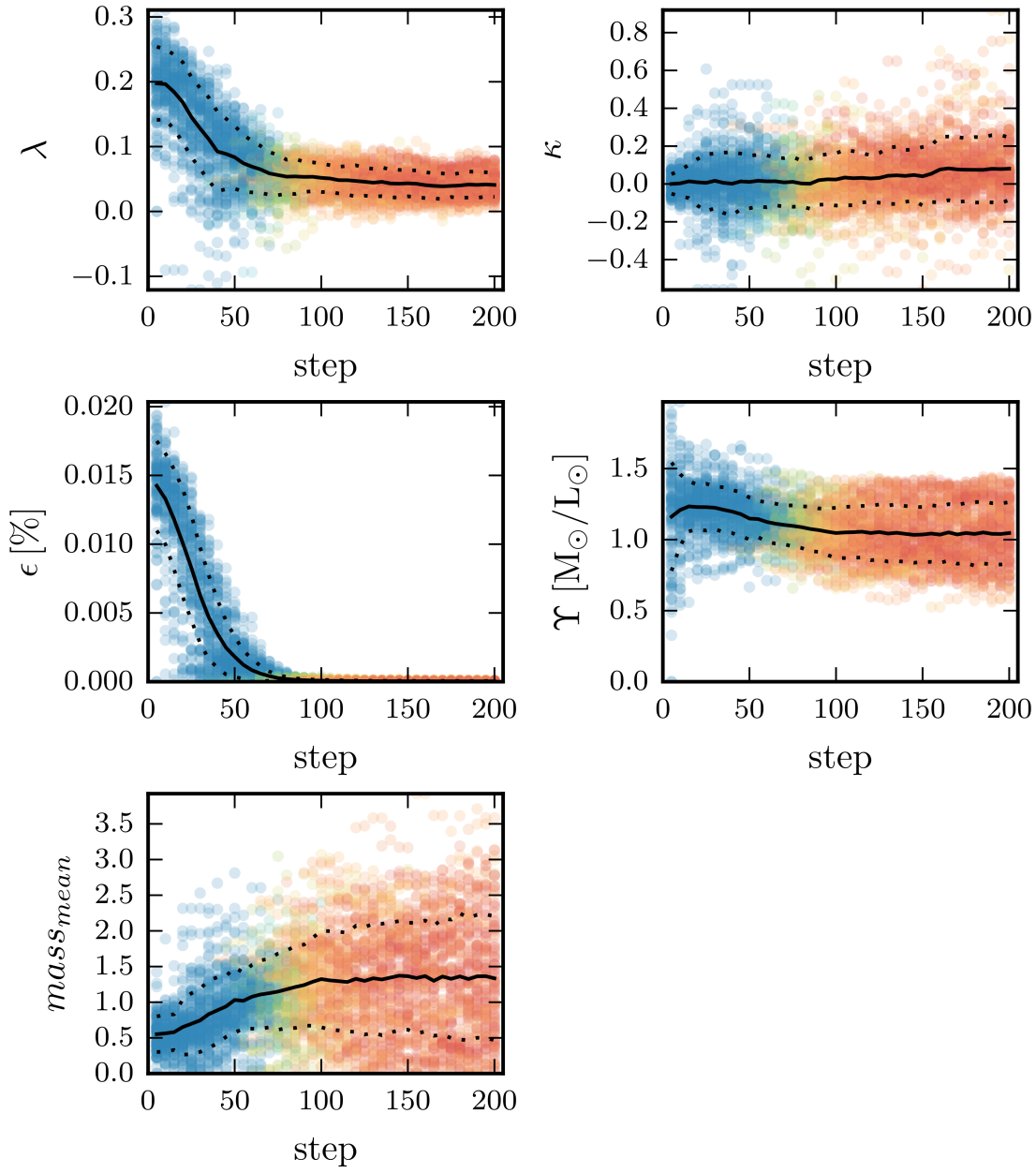

Figure 8: As in the the previous case, chain is pretty dispersed, and the value found for anisotropy is lower than what would be expected. It is interesting that both of these runs have close predictions. Here m_{eq} parameter is fixed to $2.M_{\odot}$.

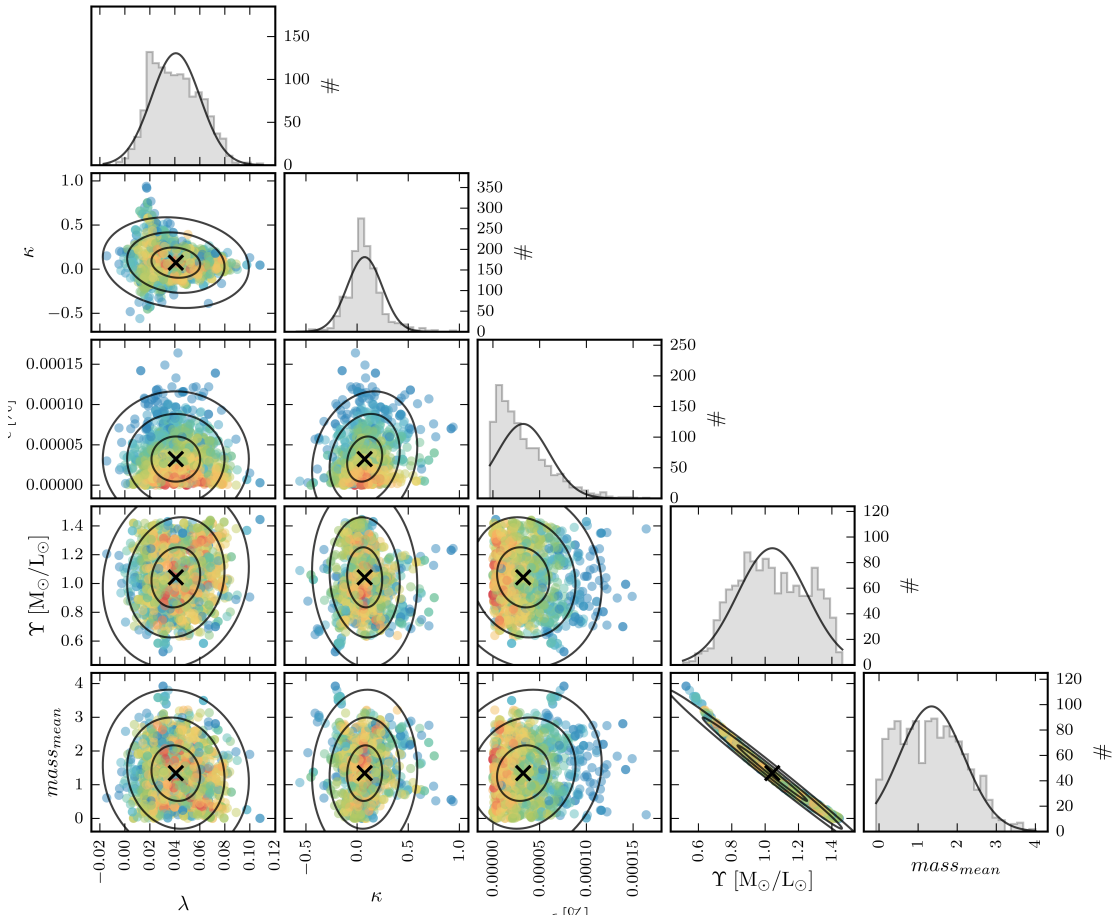

Figure 9: Distribution of the sampling marginalized.

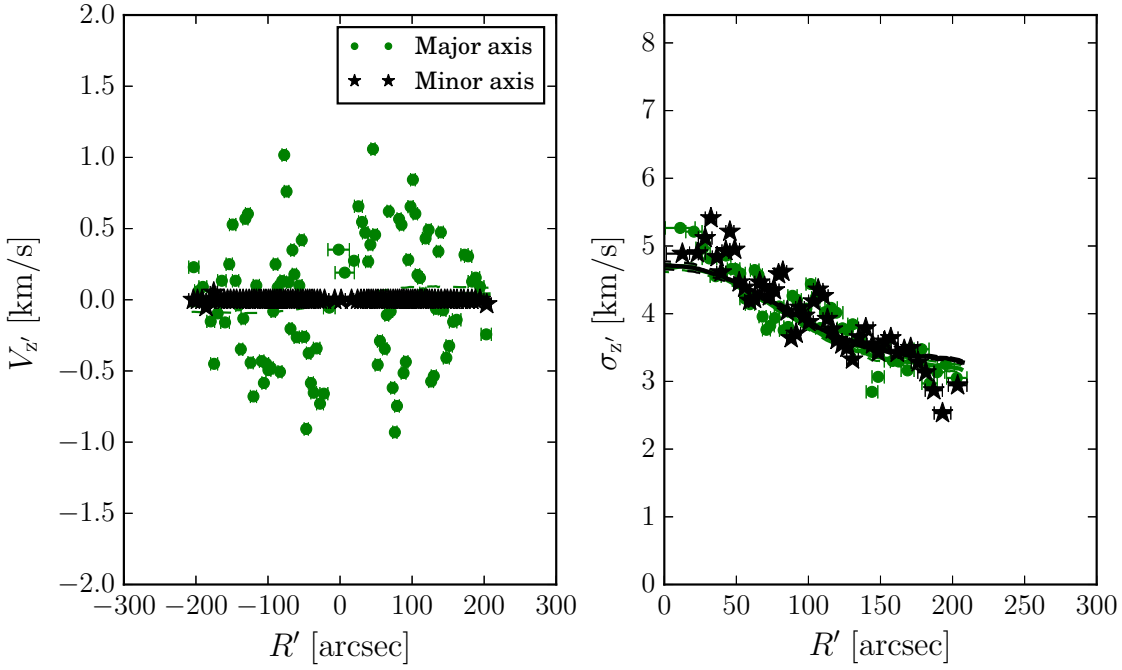

Figure 10: Overlayed input data and the model.

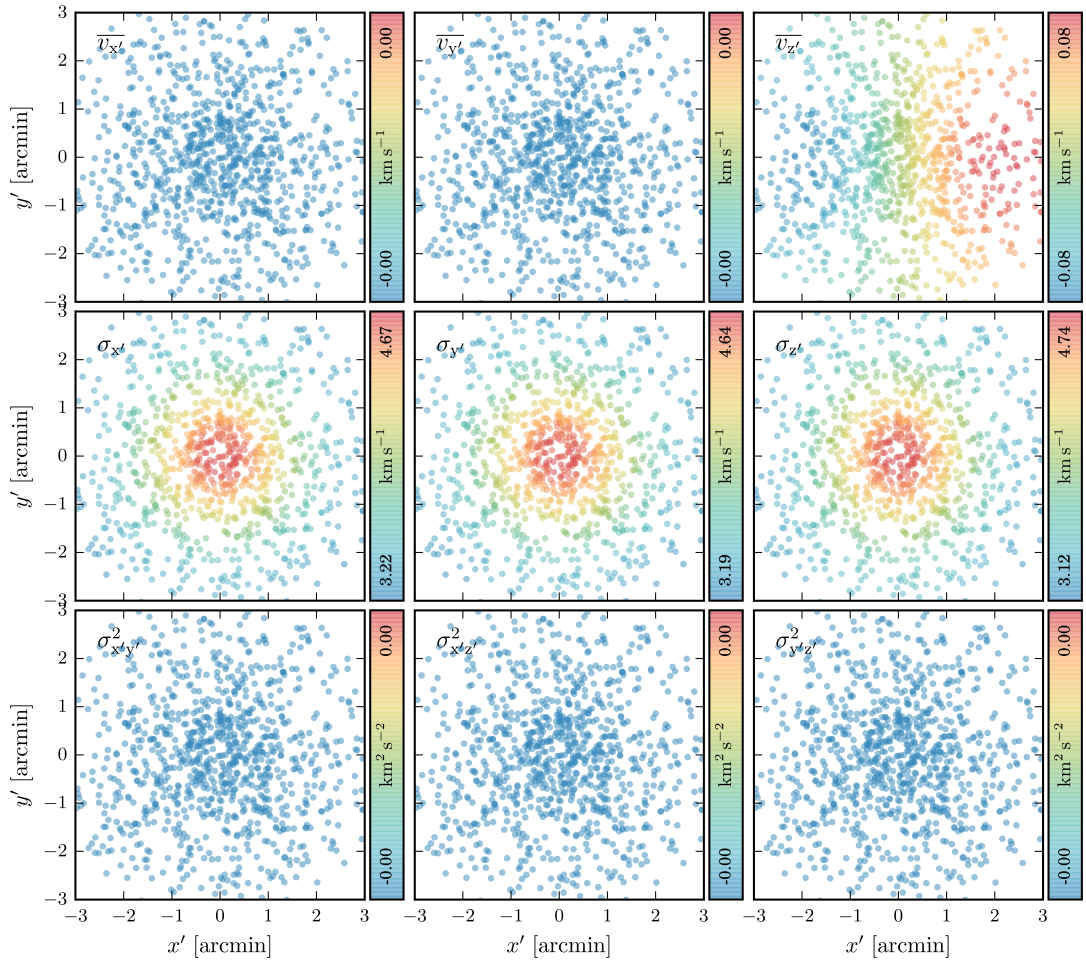
$\overline{v_{x'}}$
$\overline{v_{y'}}$
$\overline{v_{z'}}$
$\sigma_{x'}$
$\sigma_{y'}$
$\sigma_{z'}$
$\sigma^2_{x'y'}$
$\sigma^2_{x'z'}$
$\sigma^2_{y'z'}$
0.00
-0.00
0.08
-0.08
4.67
3.22
4.64
3.19
4.74
3.12
km s^{-1}
km^2 s^{-2}
y' [arcmin]
x' [arcmin]
−3 −2 −1 0 1 2 3

3.3 Run 3: Only m_{eq} is kept free and $\overline{m}$ is kept constant

In this run I have added the upper restrictions for prior probability distribution:

- m_{eq} has to be lower than $10.M_{\odot}$
- $\overline{m}$ has to be lower than $1M_{\odot}$

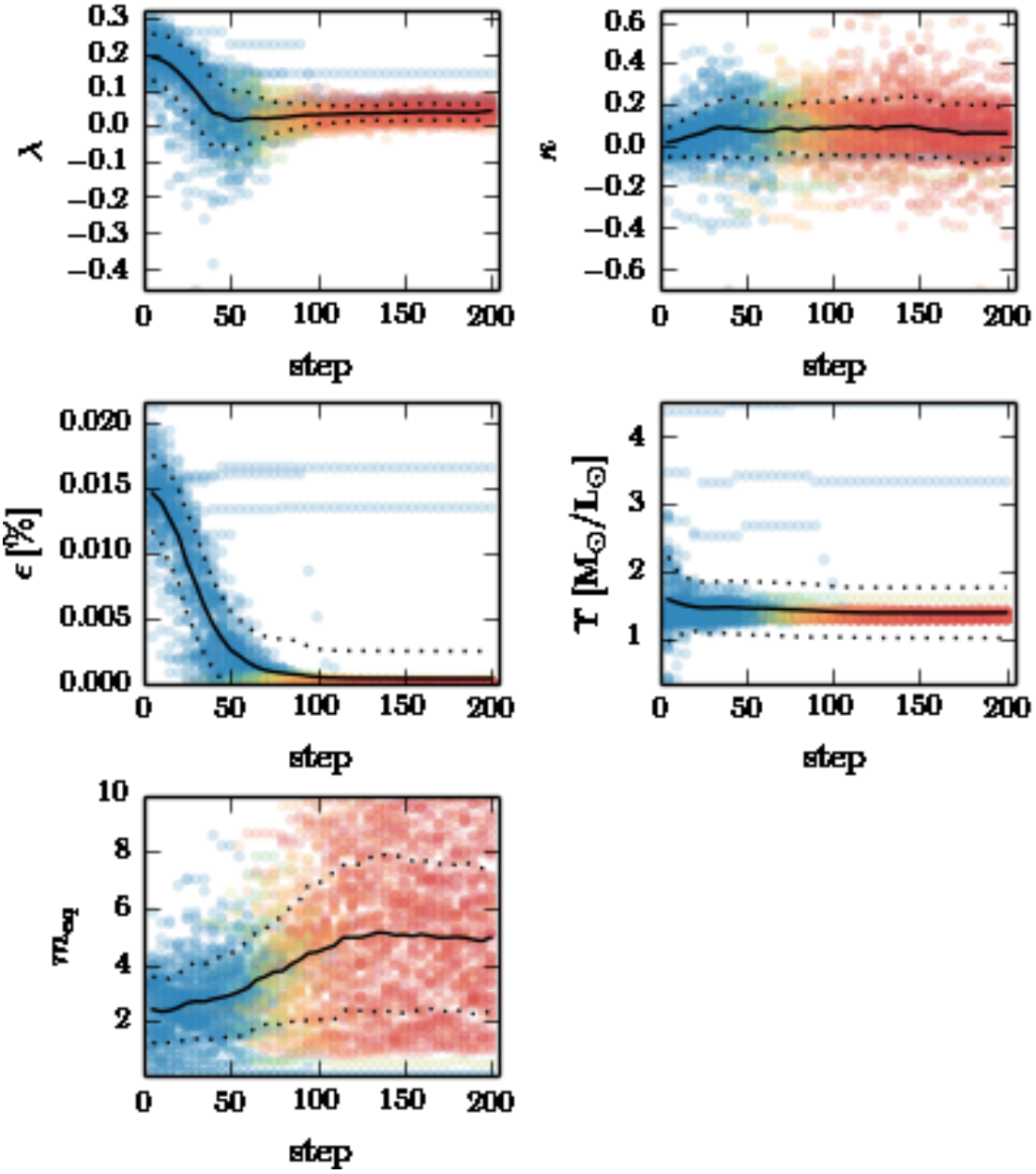

Figure 11: Again, agreement with the chains of M/L, β_z, κ and ϵ, but the chain for m_{eq} is pretty dispersed, even though there is the upper restriction. Here, the value of $\overline{m}$ is kept constant to a value of $0.15M_{\odot}$

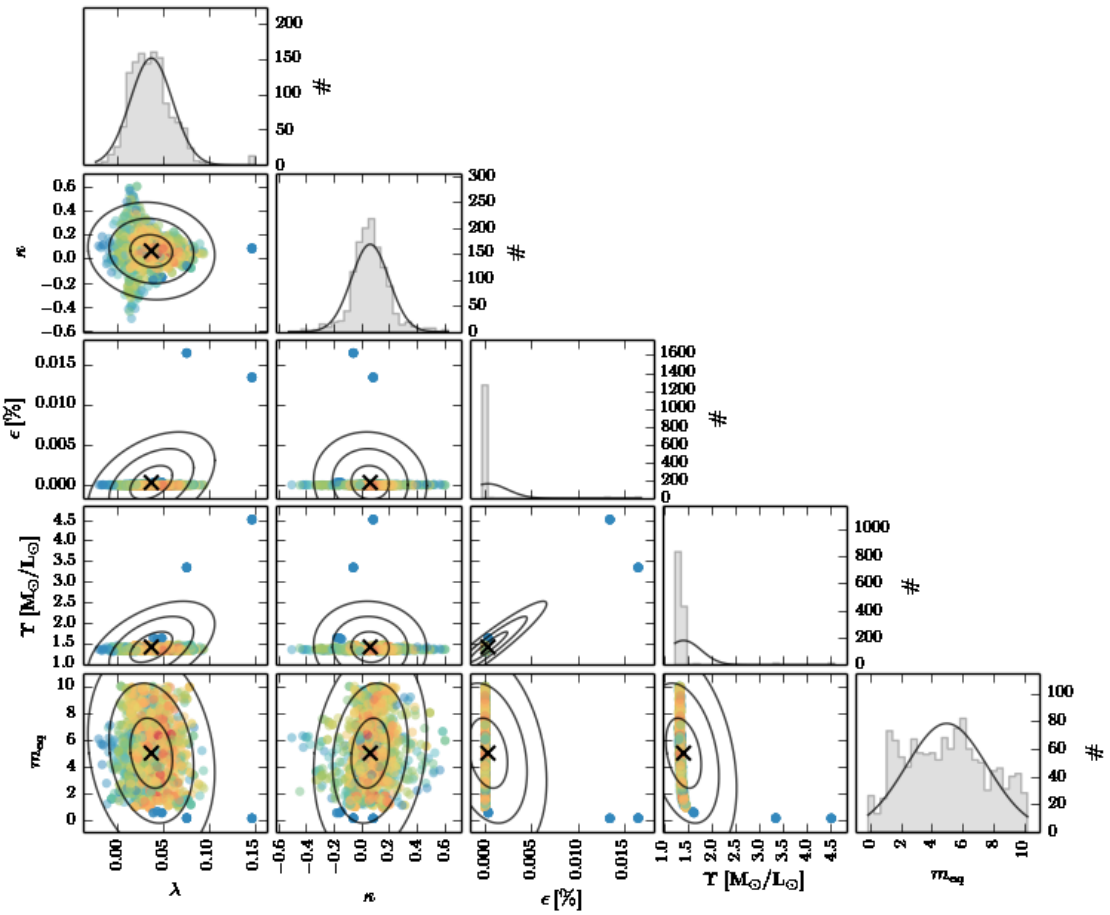

Figure 12: Distribution of marginalized sampling

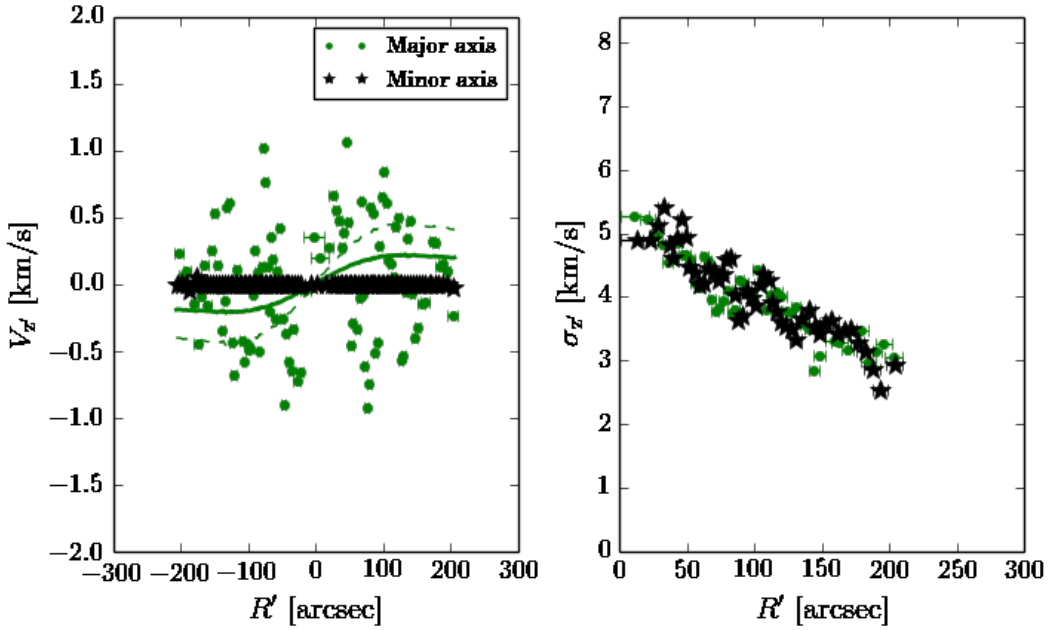

Figure 13

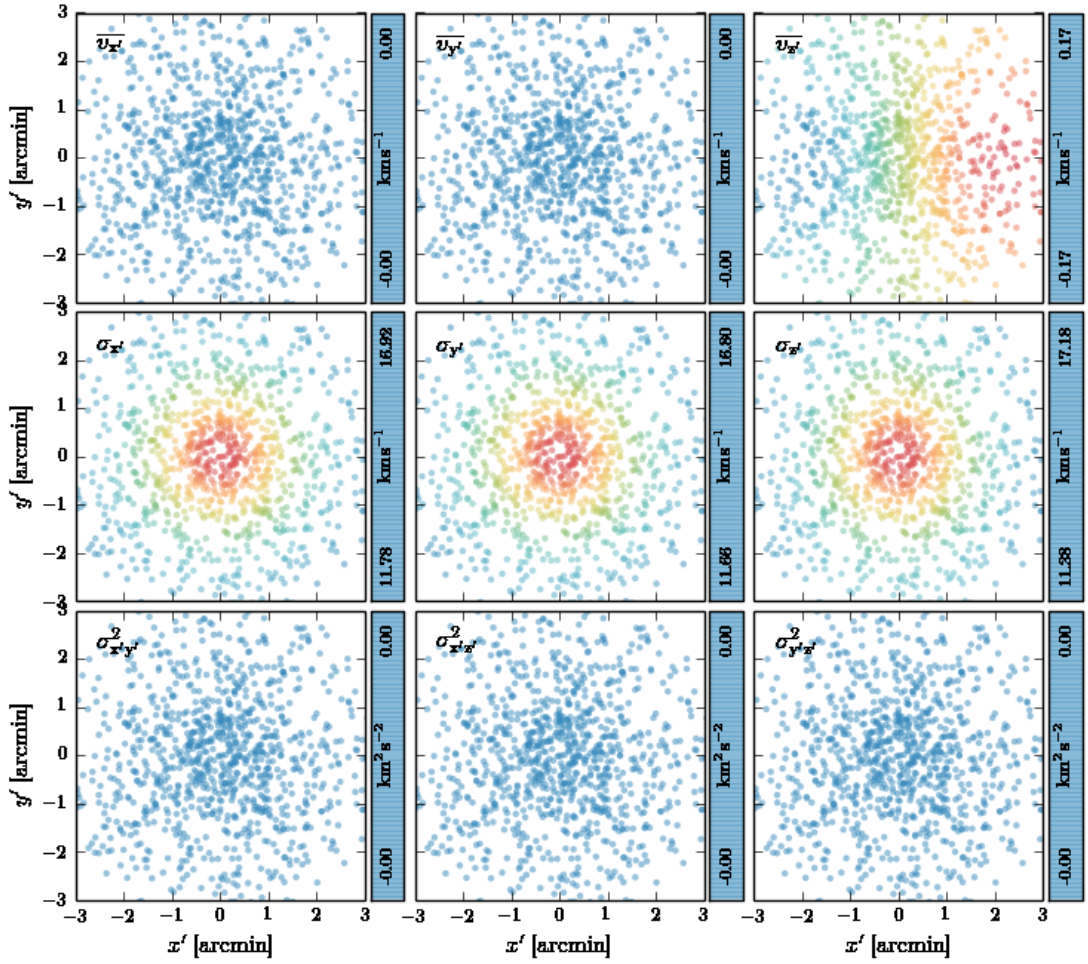
$\overline{v_{x'}}$
$\overline{v_{y'}}$
$\overline{v_{z'}}$
$\sigma_{x'}$
$\sigma_{y'}$
$\sigma_{z'}$
$\sigma^2_{x'y'}$
$\sigma^2_{x'z'}$
$\sigma^2_{y'z'}$
0.00
-0.00
0.17
-0.17
16.92
11.78
16.80
11.66
17.18
11.88
0.00
-0.00
$\mathrm{km\,s^{-1}}$
$\mathrm{km^2\,s^{-2}}$
y' [arcmin]
x' [arcmin]
−3
−2
−1
0
1
2
3

3.4 Only m_{eq} and $\overline{m}$ as free parameters with upper restrictions

Here also I have added the upper restrictions for prior probability distribution:

- m_{eq} has to be lower than $10.M_{\odot}$
- $\overline{m}$ has to be lower than $1M_{\odot}$

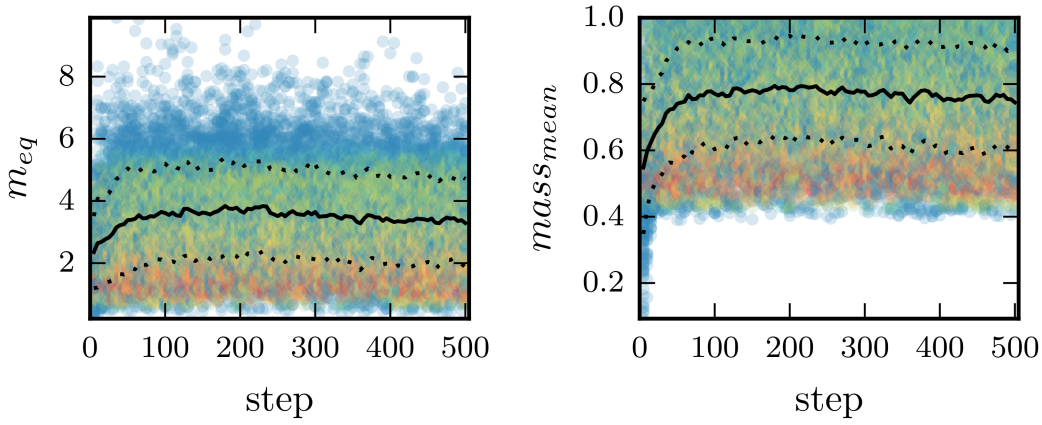

Figure 14

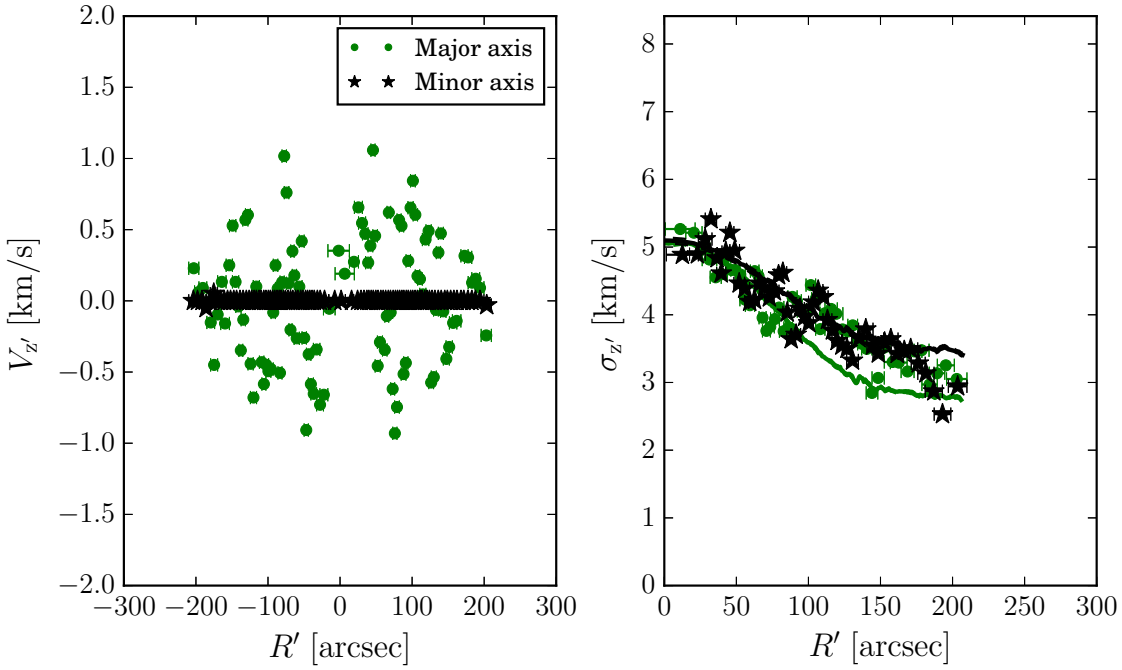

Figure 15

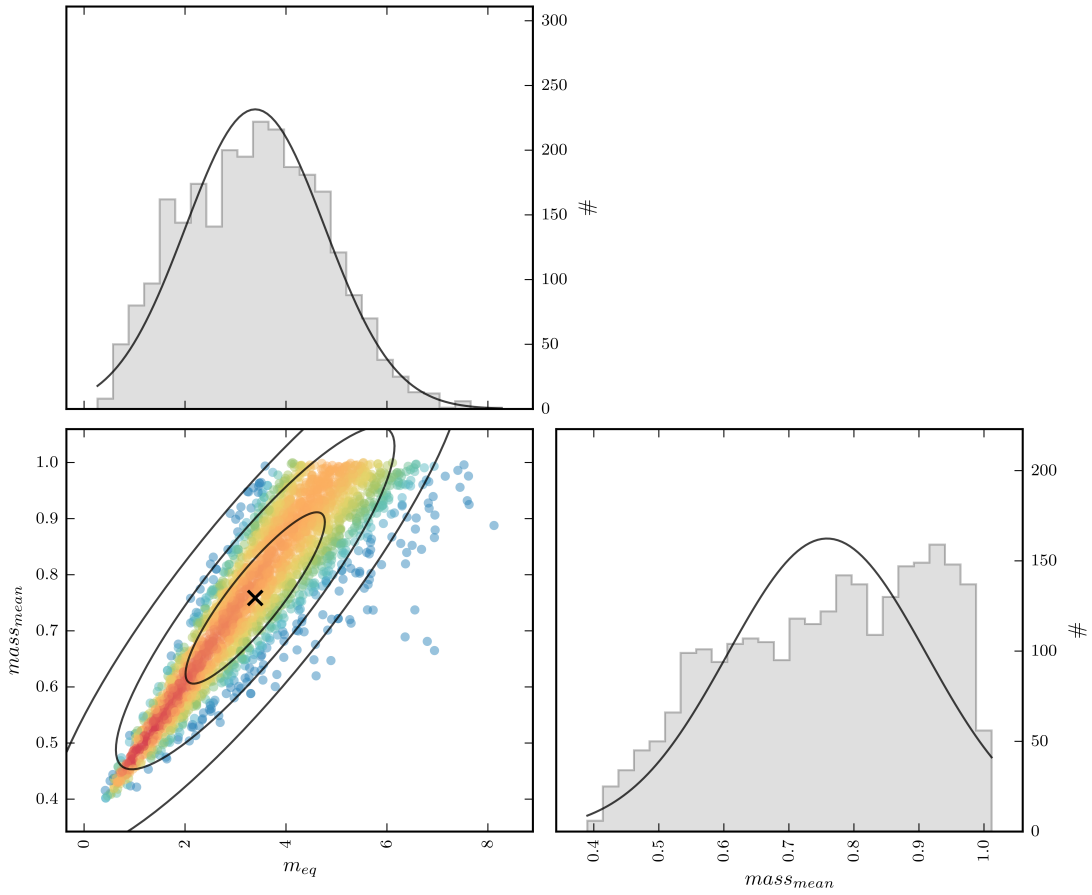
300
250
200
150
100
50
0
#
1.0
0.9
0.8
0.7
0.6
0.5
0.4
$mass_{mean}$
0
2
4
6
8
m_{eq}
200
150
100
50
0
#
0.4
0.5
0.6
0.7
0.8
0.9
1.0
$mass_{mean}$

Figure 16

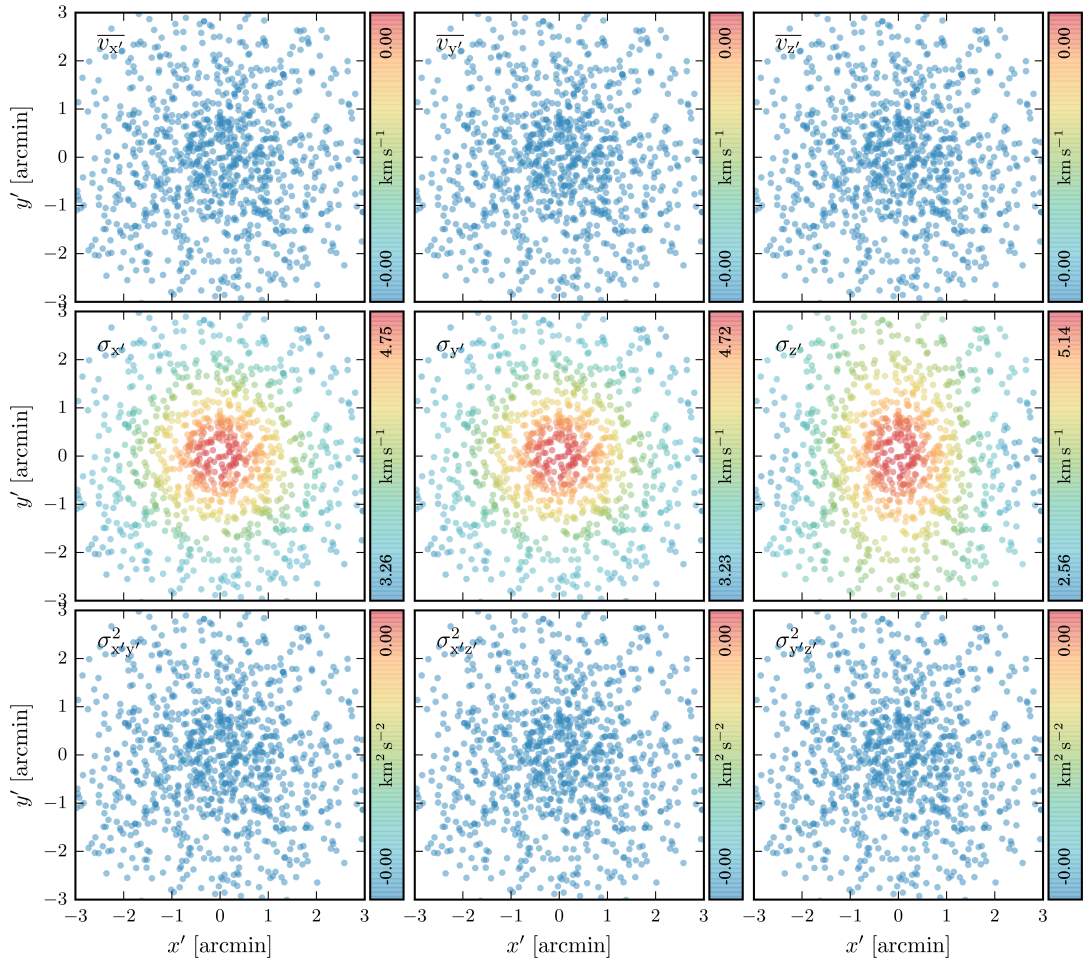

4 Questions

1. Maybe I should incorporate two kinds of calculations for the chain with `CJAM` code? One which is going to fit without equipartition formula, and the other one which is going to use the mean mass from the mass range which is reproduced the best with previous code and the m_{eq} parameter which is going to be the only free parameter ($\overline{m}$ is going to be determined from the first one, by looking at the data which is reproduced best with the model).

2. What upper restriction is physically meaningful for m_{eq} parameter?

3. In reference to the chains above, I have to ask how do we know that the eq eq. (1) is good to use? Maybe we should use it only in case that for each try of the emcee we do the procedure as described in question 1?

4. Do you have some ideas, why could the model without any correctin with Paolo's formula be so high in the center? Ling mentioned to add the surface number density, because that information could flatten, if I understood correctly?

References

[1] Bianchini, P. et al., *A novel look at energy equipartition in globular clusters*, MNRAS, vol. **458**, 2016

[2] Watkins, L. et al., *Discrete dynamical modelling of omega Centauri*, MNRAS, vol. **436**, 2013

[3] Cappellari M., *Measuring the inclination and mass-to-light ratio of axisymmetric galaxies via anisotropic Jeans models of stellar kinematics*, MNRAS, vol **390**, 2008

[4] Bellini, A. et al., *Hibble space telescope proper motion (HSTPROMO) catalogs of galactic globular clusters. I. Sample selection, data reduction, and NGC 7078 results*, Apj, vol. **797**, 2014

[5] Baldwin, A. et al., *Hubble space telescope proper motion (HSTPROMO) catalogs of Galactic globular clusters. IV. Kinematic profiles and average masses of blue straggler stars*, Apj, vol. **827**, 2016

[6] Watkins, L. et al., *Hubble space telescope proper motion (HSTPROMO) catalogs of galactic globular clusters . III . dynamical distances and mass-to-light ratios*, Apj, vol. **812**, 2015

[7] Foreman, D. et al., *emcee: The MCMC Hammer*, Astronomical Society of the Pacific, vol. **125**, 2013

[8] Trenty M., van der Marel R., *No energy equipartition in globular clusters*, MNRAS, vol, **435**, 2013

[9] Downing J. M. B., , MNRAS, vol. **407**, 2010